



## Operations Research

Publication details, including instructions for authors and subscription information:  
<http://pubsonline.informs.org>

### Transmission Capacity Allocation in Zonal Electricity Markets

Ignacio Aravena , Quentin L  t   , Anthony Papavasiliou , Yves Smeers

To cite this article:

Ignacio Aravena , Quentin L  t   , Anthony Papavasiliou , Yves Smeers (2021) Transmission Capacity Allocation in Zonal Electricity Markets. Operations Research 69(4):1240-1255. <https://doi.org/10.1287/opre.2020.2082>

Full terms and conditions of use: <https://pubsonline.informs.org/Publications/Librarians-Portal/PubsOnLine-Terms-and-Conditions>

This article may be used only for the purposes of research, teaching, and/or private study. Commercial use or systematic downloading (by robots or other automatic processes) is prohibited without explicit Publisher approval, unless otherwise noted. For more information, contact [permissions@informs.org](mailto:permissions@informs.org).

The Publisher does not warrant or guarantee the article's accuracy, completeness, merchantability, fitness for a particular purpose, or non-infringement. Descriptions of, or references to, products or publications, or inclusion of an advertisement in this article, neither constitutes nor implies a guarantee, endorsement, or support of claims made of that product, publication, or service.

Copyright    2021, INFORMS

Please scroll down for article—it is on subsequent pages



With 12,500 members from nearly 90 countries, INFORMS is the largest international association of operations research (O.R.) and analytics professionals and students. INFORMS provides unique networking and learning opportunities for individual professionals, and organizations of all types and sizes, to better understand and use O.R. and analytics tools and methods to transform strategic visions and achieve better outcomes.

For more information on INFORMS, its publications, membership, or meetings visit <http://www.informs.org>




**Crosscutting Areas**

# Transmission Capacity Allocation in Zonal Electricity Markets

 Ignacio Aravena,<sup>a,\*</sup> Quentin Lété,<sup>b</sup> Anthony Papavasiliou,<sup>b</sup> Yves Smeers<sup>b</sup>
<sup>a</sup>Lawrence Livermore National Laboratory, Livermore, California 94550; <sup>b</sup>Center for Operations Research and Econometrics (CORE), Université catholique de Louvain, 1348 Louvain-la-Neuve, Belgium

\*Corresponding author

**Contact:** aravenasolis1@llnl.gov,  <https://orcid.org/0000-0003-4837-3466> (IA); quentin.lete@uclouvain.be,

 <https://orcid.org/0000-0002-4016-0928> (QL); anthony.papavasiliou@uclouvain.be,  <https://orcid.org/0000-0002-2236-2251> (AP); yves.smeers@uclouvain.be,  <https://orcid.org/0000-0003-4312-6175> (YS)

**Received:** December 25, 2018

**Revised:** May 3, 2019

**Accepted:** August 5, 2020

**Published Online in Articles in Advance:** April 26, 2021

**OR/MS Subject Classifications:** natural resources: energy; government: energy policies; programming: integer: applications; programming: large scale systems

**Area of Review:** Environment, Energy, and Sustainability

<https://doi.org/10.1287/opre.2020.2082>
**Copyright:** © 2021 INFORMS

**Abstract.** We propose a novel framework for modeling zonal electricity markets, based on projecting the constraints of the nodal network onto the space of the zonal aggregation of the network. The framework avoids circular definitions and discretionary parameters, which are recurrent in the implementation and study of zonal markets. Using this framework, we model and analyze two zonal market designs currently present in Europe: flow-based market coupling (FBMC) and available-transfer-capacity market coupling (ATCMC). We develop cutting-plane algorithms for simulating FBMC and ATCMC while accounting for the robustness of imports/exports to single element failures, and we conduct numerical simulations of FBMC and ATCMC on a realistic instance of the Central Western European system under the equivalent of 100 years of operating conditions. We find that FBMC and ATCMC are unable to anticipate the congestion of branches interconnecting zones and branches within zones and that both zonal designs achieve similar overall cost efficiencies (0.01% difference), whereas a nodal market design largely outperforms both of them (5.09% better than FBMC). These findings raise the question of whether it is worth it for more European countries to switch from ATCMC to FBMC, instead of advancing directly toward a nodal market design.

**Funding:** This work was supported by the Bauchau Family, Bauchau Prize 2017; Université catholique de Louvain, Fonds Spécial de Recherche; the U.S. Department of Energy through the Lawrence Livermore National Laboratory [Contract DE-AC52-07NA27344]; Engie Chair in Energy Economics and Energy Risk Management; and Fonds de la Recherche Scientifique (FNRS) through a Research Fellow (Aspirant) fellowship.

**Supplemental Material:** The electronic companion is available at <https://doi.org/10.1287/opre.2020.2082>.

**Keywords:** electricity markets • robust programming • cutting plane algorithms • policy analysis

## 1. Introduction

Zonal electricity markets schedule production and consumption in power systems using a simplified zonal representation of the underlying nodal electrical network. The zonal aggregation of the grid allows market participants to trade freely within each zone and to export/import energy to/from other zones up to certain technical limitations. Two approaches toward zonal market design are the focus of this paper, both of which currently coexist in the European electricity market:

1. Imposing limitations on the cross-border exchanges between pairs of neighboring zones and
2. Imposing limitations on the configuration of net positions (i.e., exports – imports) of zones.

The first approach is known as available-transfer-capacity market coupling (ATCMC) (APX Group et al. 2010). Available transfer capacity (ATC) refers to the capacity of the interconnectors between pairs of

zones. The second approach is known as flow-based market coupling (FBMC) (50Hertz et al. 2017). The term “flow-based” (FB) refers to the fact that FBMC mimics, at a zonal level, how electricity flows through the grid.

In FBMC, the export/import capacities of each zone are allocated implicitly, potentially capturing interdependencies between cross-border exchanges. Such interdependencies are ignored in ATCMC. Additionally, FBMC can handle a larger variety of constraints on interzonal exchanges than ATCMC, thereby allowing transmission system operators (TSOs) to include transmission constraints in a more transparent and explicit manner for day-ahead market clearing. Consequently, under FBMC, TSOs may not need to consider large security margins on cross-border exchanges.

The expected benefits of FBMC rendered it as the preferred method for linking markets in the European Union (EU). This decision was ratified by Regulation (EU) 2015/1222; it led to the implementation of

FBMC in the Central Western European (CWE) system, comprising Austria, Belgium, France, Germany, Luxembourg, and the Netherlands, in May 2015.

Despite their differences, FBMC and ATCMC are both zonal electricity markets; as such, they can only approximate the inter- and intrazonal power flows of the real grid to a limited extent. This often causes market-clearing schedules that would result in overloaded transmission equipment under both FBMC and ATCMC. Congestion management measures are required after the clearing of the electricity market, in order to operate the system within its security limits in real time. The cost of these remedial measures can be very important; however, it is commonly ignored in market analyses. For instance, the parallel run between FBMC and ATCMC for the CWE (Amprion et al. 2015) found potential welfare gains of FBMC over ATCMC in the order of €95 million for 2013 while ignoring congestion management costs. These costs amounted to €945 million in 2015, the first year of operations under FBMC (ENTSO-E 2018b). Therefore, by virtue of the magnitude of congestion management costs, the effect of these remedial actions could have affected the conclusions of the parallel run. Our aim, in this paper, is to overcome this and other common simplifications in the analysis of zonal markets by the development of models and algorithms capable of quantifying more accurately for the overall performance of different market designs and allowing for comprehensive policy analyses.

### 1.1. Historical Context

The European zonal electricity market directly inherited some of its major characteristics from the Nordic system (Norway, Sweden, Finland, and Denmark). Both are based on a decomposition of the market into zones connected by aggregated representations of the lines of the network. The decomposition into zones first reflected national borders. The day-ahead market is a pure energy market run by a power exchange (PX), which is seen as the spot market, that is, the last stage at which electricity is traded and according to which financial instruments are settled. The inevitable deviations between the day ahead and real time are treated by a special mechanism, initially run by national TSOs, that was only progressively integrated among them. Notwithstanding the integration of the energy market through a single PX, the management of the grid remains zonal. Redispatching is the main tool for dealing with congestion management in the Nordic system, but TSOs can also rely on the so-called “market splitting” to deal with intrazonal congestion. This property was only systematically used by Norway, but the EU competition authorities forced it on Sweden when the latter had difficulties managing congestion on a line to Denmark.

Other regions of the world have also implemented zonal markets. Australia is a case in point that one might want to compare with Europe insofar as the markets of the different states each form an area connected to the neighboring states by transport capacities. The zones are fixed and determined by the state borders. Zonal markets also flourished in the United States but soon gave way to nodal organizations. Peco, in Pennsylvania, was the first example of a zonal market: it was created in 1997 but collapsed after a year because of dispatching difficulties. The zonal system was one of the causes of the meltdown of the first California restructured market, which was subsequently replaced by a nodal market. Finally, the Electric Reliability Council of Texas (ERCOT) was the last attempt to install a zonal market in the United States. Here, too, redispatching costs exploded compared with what was initially planned and ERCOT moved to a nodal model. Other restructured U.S. systems immediately adopted the nodal framework.

The first trilateral version of the European market, coupling Belgium, France, and the Netherlands, came live in November 2006 (APX Group et al. 2006) as a zonal system. This was possibly inspired by the Nordic experience and the careful mix of integration and remaining national identities. It has since developed to encompass the whole European continent, including the Nordic countries. However, the European zonal system did not resort to market splitting (except in the Nordic countries) but to a construction of “cross-border” capacities initially exposed in Regulation (EC) 2003/1228. The zones correspond to member states (which can be as large areas as France and Germany or as small as Belgium) and are thus based on a political configuration rather than a technical or economic analysis. Congestion is fully managed by redispatch. Although the zonal system is enshrined in legislation, including Regulation (EC) 2003/1228, Regulation (EC) 2009/714, and Regulation (EC) 2015/1222, one cannot exclude that the evolution may end up being more in line with what happened in the United States. The reasons are technical. Well before restructuring, a common Nordic argument was that the Nordic transmission system had been designed for north-south transport (at the time Danish coal in the south and hydro in the north). The argument remains valid today but in a different form (Danish renewable power in the south and storage in the north). Unscheduled flows were thus not a main issue, given the largely radial grid structure. But neither the EU grid nor the U.S. system were designed in such a radial fashion, with the consequence that unscheduled flows and congestion may turn out to be more important. Also, although the Nordic system exploited zone splitting effectively in Norway in order to relieve the recourse to redispatching, the EU has so far always resisted resorting to smaller zones that could

help when a single price zone contains congested “critical infrastructure.” For instance, the recent bidding zone review performed by the European system operators recognized that the current configuration is inefficient; however, the review failed to suggest recommendations for improving the bidding zone delimitation (ENTSO-E 2018a, ACER 2019). Recalling the ERCOT experience when redispatching costs had been dismissed as irrelevant before they blew up a few years later, one can only note that these costs that were deemed to remain below €45 million/year in Germany (2007, maximum prior to market coupling) now (2017) amount to €1,161 million/year in that country (ENTSO-E 2018b). Finally, it is worth mentioning that, apart from these efficiency effects, a zonal market followed by redispatching introduces cross-subsidies from consumers to generators and between member states.

The models presented in this paper are intended to provide an instrument to understand the possible evolution of the zonal system. These models avoid simplifying assumptions often made in economic analyses and aim at being as realistic as possible in their encompassing of current and future legal obligations. The day-ahead market follows the organization described in Regulation (EC) 2009/714. Real-time operation, which is only currently defined in Regulation (EC) 2015/1222 and Regulation (EU) 2017/2195 stating legal objectives, assumes that these objectives are effectively realized. The price to pay for this lack of simplification is computational, both in terms of algorithmic tools as well as machine resources.

A European model can only be idiosyncratic because of its peculiar institutions. But with its coverage of 989 GW (ENTSO-E 2017), and about 500 million consumers (Eurostat 2018), the European market is significantly larger than all the restructured U.S. markets (CAISO 60 GW, ERCOT 75 GW (FERC 2018)) and also than the largest U.S. regional transmission organizations (RTOs) like PJM (166 GW (FERC 2018)) and MISO (174 GW (FERC 2018)). It can also be noted that the current European market organization introduces systematic discrepancies between the day-ahead and real-time representations of the system that are much deeper than the differences present in nodal market organizations, which have been affecting some of the essential tools of U.S. markets, such as virtual trading. The methodology adopted here can be, if not directly transposed, at least adapted to examine the impact of phenomena, such as the effect of unit commitment or transmission switching decisions on prices (Hogan 2016), which interrupt the normal mechanism of arbitrage between day ahead and real time in U.S. markets.

## 1.2. Literature Review

Owing to political and institutional constraints, the EU market carries a legacy market design that is characterized by a geographical and functional segmentation of short-term operations that are interdependent and that can and should be co-optimized. The most notable consequences of this legacy market design are (i) the separation of reserve and energy clearing in day-ahead markets, (ii) the absence of a real-time market for reserve capacity, (iii) the reduced coordination of TSOs across geographic borders in real time, (iv) the artificial segmentation of real-time operations into congestion management and balancing, and (v) zonal pricing in the day ahead. There are numerous short-term and long-term inefficiencies and price formation barriers that result from this segmentation (Papavasiliou et al. 2019). These inefficiencies are becoming increasingly difficult to handle in a regime of large-scale renewable energy and distributed resource integration, which commands improved spatiotemporal coordination at the transmission and distribution level.

The separation of reserve and energy clearing in the day ahead impedes the accurate formation of forward reserve prices, because balancing service providers need to anticipate energy prices that dictate their opportunity cost for offering reserve, a function that is performed automatically in co-optimization. The absence of a real-time market for reserve capacity undermines the creation of a favorable environment for investing in operating reserve capacity, because it becomes extremely challenging to value reserve accurately based on real-time scarcity. Reduced real-time coordination makes it challenging for zones to share low-cost renewable resources across borders, when this supply becomes unexpectedly available in real time. The artificial segmentation of congestion management and balancing in real time is likely to result in conservative allocation of transmission capacity in the emerging EU balancing platforms (PICASSO and MARI) in order to avoid security violations in real time. Zonal pricing in day-ahead operations results in inefficient commitment decisions of inflexible resources. The present paper does not aim at quantifying all of these effects simultaneously. Instead, the goal is to isolate the effect of zonal pricing on inefficient day-ahead unit commitment (item (v)). We therefore focus the literature review and model on this specific topic and refer the reader to Papavasiliou et al. (2019) for a broader discussion and comparison of the impact of the aforementioned legacy market design features on short- and long-term efficiency.

ATCMC has been the standard zonal electricity market model analyzed in the literature because of its past presence in U.S. electricity markets and its



current presence in European electricity markets. Studies using small examples and realistic systems, under various assumptions and modeling choices, have all concluded that the performance of ATCMC is significantly worse than that of a nodal system (see Aravena and Papavasiliou 2017) and references therein for a survey), even in the case where ATCs can be optimized so as to reduce real operation costs (Jensen et al. 2017).

Academic studies on FBMC, on the other hand, are scarce as FBMC is a relatively new capacity allocation methodology. Early studies were performed before the *go-live* of FBMC at the CWE. Waniek et al. (2010) study the day-ahead market performance and the accuracy of power flow approximations of ATCMC, FBMC and the nodal design. For ATCMC and FBMC, the authors disaggregate zonal injections into nodal injections in proportion to the injections in a base case (similar to the procedure followed by RTE, see 50Hertz et al. 2017). The factors that are used for disaggregating zonal injections into nodal injections are known as generation shift keys (GSKs) in the literature. The study finds that FBMC outperforms ATCMC in terms of both performance and accuracy, whereas the nodal design exhibits superior performance relative to both FBMC and ATCMC. Following the *go-live*, in an effort toward understanding the new capacity allocation mechanism, Van den Bergh et al. (2016) summarize the concepts and methodology used in FBMC.

Significant attention has been dedicated toward studying how discretionary parameters determined by TSOs affect the day-ahead outcome of FBMC. Marien et al. (2013) study the effect of the configuration of bidding zones and the determination of flow reliability margins<sup>1</sup> and GSKs on exchanges and prices. The authors find that different choices for these parameters for the same system can lead to very different market outcomes. In the same vein, Dierstein (2017) analyses different strategies used by CWE TSOs to compute GSKs and how they affect the outcome of FBMC and congestion management for cross-border lines. The author finds that dynamic GSK strategies (i.e., where GSKs vary from one hour to the next) outperform static GSK strategies, the latter being currently used by all TSOs except RTE.

### 1.3. Contributions and Paper Organization

The contributions of the present paper are threefold. In terms of modeling, we propose a framework for modeling zonal electricity markets that avoids the discretionary parameters and circular definitions (i.e., definitions of parameters that depend on a base case) present in the current practice and in the literature. This is achieved in the proposed FBMC and ATCMC models by projecting the actual network constraints onto the

space of zonal net positions and cross-border exchanges, respectively. The computational contribution of the paper is the development of cutting-plane algorithms for clearing the day-ahead market under each policy, while endogenously enforcing robustness of the import/export decisions against single-element contingencies (i.e., satisfying the N-1 security criterion, see RTE 2019, APX Group et al. 2010, 50Hertz et al. 2017). The N-1 security criterion is an essential attribute that needs to be accounted for in the modeling of the European day-ahead market. The resulting clearing problems correspond to adjustable robust optimization problems (Ben-Tal et al. 2009). The policy contribution of the paper is the detailed simulation of a realistic-scale instance of the CWE system (Aravena and Papavasiliou 2017) against detailed models of the nodal design, FBMC, and ATCMC. These simulations account for the clearing of energy and reserves, renewable supply forecasts errors and the outage of components, the pricing of nonconvex operating costs and constraints, and the two-stage nature of market operations whereby day-ahead market clearing is followed by congestion management and balancing. Numerical results over the equivalent of 100 years of operating conditions demonstrate that FBMC and ATCMC attain very similar performance. The major policy message of the paper is to challenge whether it is worth it for more European countries to switch from ATCMC to FBMC, instead of advancing directly to a nodal design.

The paper is organized as follows. Section 2 introduces our modeling framework for transmission capacity allocation in zonal markets using linear programs that capture the most important differences in the alternative market designs. These simplified models permit an analysis of the differences with respect to the nodal design and the FBMC methodology implemented in the CWE. Section 3 develops cutting-plane algorithms for simulating the nodal design, FBMC, and ATCMC under the N-1 security criterion. Section 4 presents the large-scale CWE system used in the realistic case study, and Section 5 presents the main numerical results and discusses the implications of these results for zonal electricity markets. Finally, Section 6 concludes the paper and outlines directions for future research.

## 2. Transmission Capacity Allocation in Electricity Markets

Transmission capacity allocation mechanisms include (i) forward contracts, for instance, the long-term auctions carried out by the Joint Allocation Office (2015) and (ii) different types of implicit allocation, typically used in day-ahead electricity markets (Schweppe et al. 1988). In the following, we focus on day-ahead electricity markets and describe each policy for transmission

capacity allocation (nodal, FBMC, and ATCMC) in its simplest form in order to better understand the differences between them. We adopt the following assumptions: (i) demand is fixed and only producers bid in the market, (ii) all market participants act as price-takers (i.e., they bid their true cost to the market), and (iii) all energy is traded in the day-ahead auction (i.e., we ignore long-term contracts and bilateral trades). The latter implies that we also ignore the intraday market. This assumption is adopted in order to simplify the analysis. However, we note that the intraday markets are also organized as zonal markets and therefore are exposed to the same inefficiencies stemming from the inaccurate representation of the transmission network as zonal day-ahead markets.

### 2.1. Nodal Electricity Markets

Nodal electricity markets use locational marginal pricing (LMP), first proposed by Schweppe et al. (1988), in order to price electricity at every node of the system, while accounting for transmission congestion in a direct current approximation of the alternating current network equations. Under our assumptions, the LMP day-ahead market can be cleared by solving the optimization problem (1)–(3):

$$\begin{aligned} \min_{v \in [0,1], f, \theta} \quad & \sum_{g \in G} P_g Q_g v_g, & (1) \\ \text{s.t.} \quad & \sum_{g \in G(n)} Q_g v_g - \sum_{l \in L(n, \cdot)} f_l + \sum_{l \in L(\cdot, n)} f_l = Q_n \\ & \forall n \in N \quad [\rho_n], & (2) \\ & -F_l \leq f_l \leq F_l, f_l = B_l(\theta_{m(l)} - \theta_{n(l)}) \quad \forall l \in L. & (3) \end{aligned}$$

The notation in this model is as follows:  $Q_g, P_g$  correspond to the quantity and price bid by generator  $g \in G$ ;  $G(n)$  is the set of generators at node  $n$ ;  $Q_n$  is the forecast demand at node  $n \in N$ ;  $F_l, B_l, m(l), n(l)$  are the thermal limit, susceptance, and adjacent nodes (in the outgoing and incoming direction, respectively) of line  $l \in L$ ;  $L(m, n)$  is the set of lines directed from node  $m$  to node  $n$ ;  $v_g$  is the acceptance/rejection decision for the bid placed by generator  $g$ ;  $f_l$  is the flow through line  $l$ ; and  $\theta_n$  is the voltage angle at node  $n$ .

The objective function (1) corresponds to the total operation cost; Constraint (2) enforces nodal power balance; and Constraint (3) models the direct current transmission constraints. Prices  $\rho_n$  can be obtained as the dual multipliers of Constraint (2).

Note that we use the acceptance level  $v_g$  as a decision variable, following academic literature related to European electricity markets (Van den Bergh et al. 2016, Aravena and Papavasiliou 2017). This differs from the formulation that represents the output of generators as decision variables and is more common in the literature related to nodal markets. The formulation that we employ here offers the advantage that its linear

programming dual has as a variable the surplus of each bid/generator, unscaled, which is useful when enforcing pricing restrictions for discrete bids (see Section EC.3 of the electronic companion). In addition, we use the B-theta formulation instead of the one based on power transfer distribution factors (PTDF). The B-theta formulation is more convenient for representing line contingencies, as we discuss in Section 3.1.

The LMP policy implicitly allocates the capacity of all lines in the system, without any distinction between zones, and while respecting the network constraints. This implies that, absent any uncertainty (such as renewable energy forecast errors or outages), the optimal acceptance/rejection decisions  $v^*$  can be implemented directly in the system without violating any technical constraint.

### 2.2. Zonal Electricity Markets

In zonal electricity markets, electricity is priced at a zonal level and nodal level information is discarded (Ehrenmann and Smeers 2005). Bids are associated with zones instead of nodes, and transmission constraints can only be imposed at a zonal level. A zonal market can be cleared by solving problem (4)–(6):

$$\begin{aligned} \min_{v \in [0,1], p} \quad & \sum_{g \in G} P_g Q_g v_g, & (4) \\ \text{s.t.} \quad & \sum_{g \in G(z)} Q_g v_g - p_z = \sum_{n \in N(z)} Q_n \quad \forall z \in Z \quad [\rho_z], & (5) \\ & p \in \mathcal{P}, & (6) \end{aligned}$$

where  $p_z$  corresponds to the net position of zone  $z \in Z$ ,  $G(z), N(z)$  correspond to the set of generators and nodes in zone  $z$ , and  $\mathcal{P}$  corresponds to the feasible set of net positions. The set  $\mathcal{P}$  is a convex polyhedron that is defined differently for each interzonal capacity allocation mechanism but always respects power balance, that is,  $\sum_z p_z = 0$ . In this model, Constraint (5) defines the zonal net positions, and Constraint (6) enforces that the zonal net positions belong in  $\mathcal{P}$ .

European regulations set forth guidelines for defining  $\mathcal{P}$ . Annex I of Regulation (EC) 2009/714 establishes that transmission system operators (TSOs) “shall endeavour to accept all commercial transactions, including those involving cross-border-trade . . .” (Article 1.1) and that “. . . TSOs shall not limit interconnection capacity in order to solve congestion inside their own control area, save for the abovementioned reasons and reasons of operational security . . .” (Article 1.7). At the same time, Regulation (EU) 2015/1222 requires allocated cross-border capacity to be firm (Article 69).<sup>2</sup> In the spirit of these regulations,  $\mathcal{P}$  should include all net position configurations  $p$  that are feasible with respect to the real grid and exclude those that can be proven to lead to unsafe operating conditions. We describe three methodologies for defining  $\mathcal{P}$ : FB with GSKs, FB with exact projection, and ATC with exact projection.

### 2.2.1. Flow-Based Methodology with Generation Shift Keys.

This methodology is currently used in the implementation of FBMC in the CWE (50Hertz et al. 2017). The first step in the method is to determine GSKs for each generator within each zone. GSKs quantify the change in the output of generators that would result from a change in zonal net positions with respect to a base case dispatch, that is,  $GSK_g = Q_g \Delta v_g / \Delta p_{z(g)}$ . GSKs, along with the node-to-line PTDF matrix, are used to compute zone-to-line PTDFs as  $PTDF_{l,z} = \sum_{g \in G(z)} GSK_g \cdot PTDF_{l,n(g)}$ ,  $\forall l \in L, z \in Z$ . Here,  $n(g)$  corresponds with the node at which generator  $g$  is located, and  $PTDF_{l,n}$  is the power transfer distribution factor of line  $l$  and node  $n$ . Zone-to-line PTDFs are the equivalent of node-to-line PTDFs when the nodes are aggregated into zones. Their computation, however, is more challenging: one needs to assume how an additional injection of 1 MW in a zone decomposes into nodal injections in that zone (which is exactly the role of GSKs). Then, using the base case dispatch (denoted with a zero superscript), the flow across each line is approximated as  $f_l \approx f_l^0 + \sum_{z \in Z} PTDF_{l,z} \cdot (p_z - p_z^0)$ ,  $\forall l \in L$ .

If, for a certain line  $l \in L$  and any zone  $z \in Z$ ,  $PTDF_{l,z}$  is larger than 5%, then  $l$  is considered to be a critical branch (CB). For each critical branch, TSOs determine its corresponding remaining available margin (RAM) starting from the thermal capacity of the branch minus the flow on the base case ( $F_l - f_l^0$ ), subtracting the flow reliability margin, and adding the final adjustment value. Finally, the set of feasible net positions with GSKs,  $\mathcal{P}^{FB-GSK}$ , is described by

$$\mathcal{P}^{FB-GSK} = \left\{ p \in \mathbb{R}^{|Z|} \mid \sum_{z \in Z} p_z = 0, \sum_{z \in Z} PTDF_{cb,z} \cdot p_z \leq RAM_{cb} \forall cb \in CB \right\}. \quad (7)$$

We denote by FBMC-GSK the flow-based market clearing Problems (4)–(6) with  $\mathcal{P} = \mathcal{P}^{FB-GSK}$ .

The methodology has several points where discretionary decisions are made by TSOs. These include the selection of a base case, the determination of GSKs, the selection of critical branches, and the determination of flow reliability margins and final adjustment values, all of which are subject to the discretion of the TSOs. Indeed, different TSOs use different criteria for certain choices (CREG 2017, 50Hertz et al. 2017). Additionally,  $\mathcal{P}^{FB-GSK}$  will only be a good representation of reality whenever the flows on critical branches are approximated accurately. Unfortunately, this cannot be guaranteed (Wanik et al. 2010). Furthermore, a circularity problem arises: the better TSOs can anticipate the outcome of the market, the closer the base case would be to reality and, consequently, power flows would be approximated more accurately. However, the

outcome of the market depends on the parameters decided by TSOs. In addition, the definition of these parameters grants a certain degree of flexibility to the TSOs. This can lead to situations where TSOs anticipate the generation costs of the units in their control area and prevent certain net positions that correspond to unlikely generating patterns from being cleared. Not only are these practices very difficult to model but they also contravene the principle of nondiscrimination that underlies European legislation. These problems, among others, have placed the FBMC-GSK methodology under scrutiny by the National Regulatory Authorities; see Energy Markets Inspectorate (EI) and Norwegian Water Resources and Energy Directorate (2017) and CREG (2017).

### 2.2.2. Flow-Based Methodology with Exact Projection.

Instead of resorting to assumptions for approximating power flows using zonal net positions, we can determine the exact set of feasible net positions  $\mathcal{P}^{FB-EP}$  with respect to the actual grid by projecting the power flow equations onto the space of net positions:

$$\mathcal{P}^{FB-EP} = \left\{ p \in \mathbb{R}^{|Z|} \mid \exists (\bar{v}, f, \theta) \in [0, 1]^{|G|} \times \mathbb{R}^{|L|} \times \mathbb{R}^{|N|} : \right. \\ \sum_{g \in G(z)} Q_g \bar{v}_g - p_z = \sum_{n \in N(z)} Q_n \quad \forall z \in Z, \\ \sum_{g \in G(n)} Q_g \bar{v}_g - \sum_{l \in L(n, \cdot)} f_l + \sum_{l \in L(\cdot, n)} f_l = Q_n \quad \forall n \in N, \\ \left. -F_l \leq f_l \leq F_l, f_l = B_l(\theta_{m(l)} - \theta_{n(l)}) \quad \forall l \in L \right\}. \quad (8)$$

This set includes all zonal net positions for which there exists at least one vector of generator output levels that is feasible under the full network model. The set  $\mathcal{P}^{FB-EP}$  is not currently used in EU market operations. It is rather a mathematical definition of the flow-based domain that allows for an objective quantitative comparison of a very broad family of aggregation models (including FBMC and ATCMC). Indeed, as it will be shown in the next section, this definition can easily be extended to compute ATCs. Using  $\mathcal{P}^{FB-EP}$  in (6) has four main advantages over other alternatives: (i) it is a natural way to approach an aggregation model, as it corresponds to the projection of the set of feasible nodal injections to the space of zonal net positions; (ii) it does not require any assumptions or discretionary parameters; (iii) it allows all trades that are feasible with respect to the real network to be cleared; and (iv) it prevents all trades that can be proven to be impossible from being cleared. Note that implementing this approach requires information about the grid, the installed

generation capacity, and the forecast demand at each node, all of which are already available to system operators. No information about the price or attribution of the bids to nodes is necessary.

One fundamental characteristic of our proposal to use the set  $\mathcal{P}^{FB-EP}$  for zonal market clearing is that it fully separates the representation of the grid (i.e., the polytope  $\mathcal{P}^{FB-EP}$ ) from dispatch considerations. This is in contrast with the existing method that relies on GSKs, according to which the representation of the grid depends on the dispatch. It is the inclusion of the dispatch considerations in the representation of the grid that leads to a limitation of cross-border exchanges that is known to exist with the current methodology; see ACER (2018).

We note that, under the assumption that market participants bid truthfully, the quantity bid by generator  $g$  is equal to its capacity. This is why parameter  $Q_g$  appears both in the market clearing Problems (4)–(6) and in the definition of the polytope in Equation (8).

**2.2.3. Available-Transfer-Capacity Methodology with Exact Projection.** The ATC methodology defines a set of interconnectors  $T$  between neighboring zones, each  $t \in T$  comprising cross-border lines  $L(t) \subseteq L$ , and assigns a maximum capacity in the forward ( $ATC_t^+$ ) and backward ( $ATC_t^-$ ) direction for each interconnector. These capacities are determined in a series of steps, analogous to those presented in Subsection 2.2.1, aiming at computing simultaneous limits on cross-border exchanges between pairs of neighboring zones; see APX Group et al. (2010) and Aravena and Papavasiliou (2017). We abstract from these discretionary considerations and, following the principle that  $\mathcal{P}$  should include the largest possible subset of feasible net position configurations, Regulation (EC) 2009/714, we compute ATCs by solving the optimization Problems (9)–(11):

$$\max_{ATC} \prod_{t \in T} (ATC_t^- + ATC_t^+), \tag{9}$$

$$\text{s.t. } -ATC_t^- \leq ATC_t^+ \quad \forall t \in T, \tag{10}$$

$$[-ATC^-, ATC^+] \subseteq \mathcal{E}^{EP}, \tag{11}$$

where  $[-ATC^-, ATC^+] \subseteq \mathbb{R}^{|T|}$  is the rectangle with lower vertex  $-ATC^-$  and upper vertex  $ATC^+$  and  $\mathcal{E}^{EP}$ , defined in (12), is the feasible domain of cross-border exchanges:

$$\mathcal{E}^{EP} = \left\{ e \in \mathbb{R}^{|T|} \mid - \sum_{l \in L(t)} F_l \leq e_t \leq \sum_{l \in L(t)} F_l \quad \forall t \in T, \right. \\ \left. \exists p \in \mathcal{P}^{FB-EP} : p_z = \sum_{t \in T(z, \cdot)} e_t - \sum_{t \in T(\cdot, z)} e_t \quad \forall z \in Z \right\}. \tag{12}$$

Problems (9)–(11) seek to maximize the volume of the rectangle formed by the ATC values of all interconnectors, while ensuring that (i) the cross-border exchange between each pair of zones is bounded by their total interconnection capacity and (ii) the net positions at each exchange configuration within the ATC rectangle are feasible with respect to the real network constraints (TenneT 2014).

Once the ATC values are available from solving Problems (9)–(11), the feasible net position domain under the ATC methodology with exact projection,  $\mathcal{P}^{ATC-EP}$ , can be defined as

$$\mathcal{P}^{ATC-EP} = \left\{ p \in \mathbb{R}^{|Z|} \mid \exists e \in \mathbb{R}^{|T|} : p_z = \sum_{t \in T(z, \cdot)} e_t \right. \\ \left. - \sum_{t \in T(\cdot, z)} e_t \quad \forall z \in Z, \right. \\ \left. -ATC_t^- \leq e_t \leq ATC_t^+ \quad \forall t \in T \right\}. \tag{13}$$

In contrast with  $\mathcal{P}^{FB-GSK}$ , defined in (7), and  $\mathcal{P}^{FB-EP}$ , defined in (8), where we enforce zonal balance explicitly,  $\mathcal{P}^{ATC-EP}$  enforces zonal power balance implicitly, because the interconnectors define a transportation network between the zones. We use the same naming convention as for the flow-based methodology with GSKs: we denote the flow-based market clearing problem with exact projection ((4)–(6),  $\mathcal{P} = \mathcal{P}^{FB-EP}$ ) as FBMC-EP, and the available-transfer-capacity market clearing problem with exact projection ((4)–(6),  $\mathcal{P} = \mathcal{P}^{ATC-EP}$ ) as ATCMC-EP.

**2.3. Feasible Domain Comparison**

The feasible set of zonal net positions differs among policies. Denote by  $\mathcal{P}^{LMP}$  the feasible set of zonal net positions of the LMP policy. Then, by construction, we have that  $\mathcal{P}^{LMP} = \mathcal{P}^{FB-EP} \supseteq \mathcal{P}^{ATC-EP}$ , whereas  $\mathcal{P}^{FB-GSK}$  is not comparable to the previous sets. Thus, although FBMC-EP allows all possible interzonal exchange schedules, ATCMC-EP might not allow some of them; but FBMC-EP and ATCMC-EP will not allow clearing with an infeasible cross-border exchange schedule. FBMC-GSK, on the other hand, might prevent feasible net positions from being cleared and allow infeasible net positions to be cleared, as we demonstrate with a simple numerical example in Section 2.4. This implies that the current practice for FBMC, FBMC-GSK, is in direct violation of Regulation (EC) 2009/714, whereas the models that we propose, FBMC-EP and ATCMC-EP, obey European regulations.



The feasible set of acceptance/rejection of bids is another interesting point of comparison. Let us define the feasible set of acceptance/rejection of bids of each policy as

$$\begin{aligned} \mathcal{V}^{LMP} &= \left\{ v \in [0, 1]^{|G|} \mid \exists (f, \theta), (v, \theta, f) \right. \\ &\quad \left. \text{respecting (2)–(3)} \right\}, \\ \mathcal{V}^{FB-GSK} &= \left\{ v \in [0, 1]^{|G|} \mid \exists p, (v, p) \text{ respecting} \right. \\ &\quad \left. (5)–(6) \text{ with } \mathcal{P} := \mathcal{P}^{FB-GSK} \right\}, \\ \mathcal{V}^{FB-EP} &= \left\{ v \in [0, 1]^{|G|} \mid \exists p, (v, p) \text{ respecting} \right. \\ &\quad \left. (5)–(6) \text{ with } \mathcal{P} := \mathcal{P}^{FB-EP} \right\} \text{ and} \\ \mathcal{V}^{ATC-EP} &= \left\{ v \in [0, 1]^{|G|} \mid \exists p, (v, p) \text{ respecting} \right. \\ &\quad \left. (5)–(6) \text{ with } \mathcal{P} := \mathcal{P}^{ATC-EP} \right\}. \end{aligned}$$

Then, we have that  $\mathcal{V}^{LMP} \subseteq \mathcal{V}^{FB-EP} \supseteq \mathcal{V}^{ATC-EP}$ , whereas  $\mathcal{V}^{FB-GSK}$  is not comparable with the previous sets. This implies that, although FBMC-EP and ATCMC-EP are guaranteed to clear with a feasible cross-border exchange schedule  $p_z, z \in Z$ , the acceptance/rejection decisions for bids obtained by these models might not be feasible for the real network.

### 2.4. Policy Comparison Using an Illustrative Example

We compare LMP, FBMC-GSK, FBMC-EP, and ATCMC-EP using the four-node, three-zone network presented in Figure 1. We investigate cases of inter- and intrazonal scarce transmission capacity. In both cases, we solve the LMP model (1)–(3) directly and the FBMC-GSK model (4)–(6), with  $\mathcal{P} \equiv \mathcal{P}^{FB-GSK}$ , using the GSK strategy of the Belgian TSO (50Hertz et al. 2017). We solve the FBMC-EP model (4)–(6), with  $\mathcal{P} \equiv \mathcal{P}^{FB-EP}$ , by explicitly describing  $\mathcal{P}^{FB-EP}$  in the lifted space of  $\bar{v}, f, \theta$  using its definition (8). Concretely, this means that the market clearing problem is solved as one single optimization model that includes extended variables  $\bar{v}, f, \theta$ .

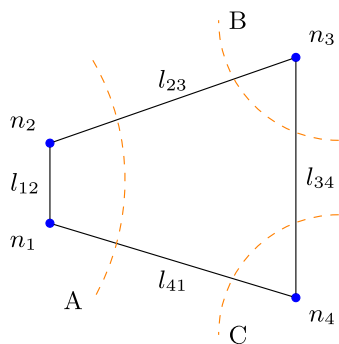
Similarly, we solve the ATC computation model (9)–(11) by explicitly modeling all vertices  $v \in \mathcal{V}$  of the rectangle  $[-ATC^-, ATC^+]$  and enforcing that the corresponding exchange limit  $e^v$  of each vertex  $v \in \mathcal{V}$  is a feasible cross-border exchange configuration, that is,  $e^v \in \mathcal{E}^{EP}$ . Here  $\mathcal{E}^{EP}$  is described on the lifted space of variables  $p^v, \bar{v}^v, f^v, \theta^v$  using its definition (12). The computed ATC values are then used to solve the ATCMC-EP model (4)–(6), with  $\mathcal{P} \equiv \mathcal{P}^{ATC-EP}$ , which is solved directly. The goal of this example is to illustrate the abstract FBMC-EP concept in a concrete setting.

**2.4.1. Interzonal Scarce Transmission Capacity.** In order to study the behavior of the different policies under interzonal scarce transmission capacity, we clear the market for the system of Figure 1 with the thermal capacity of line  $l_{41}$  assumed equal to 100 MW. All other lines are assumed to have unlimited capacity.

Table 1 presents a summary of the clearing results. We find that all zonal policies clear with acceptance/rejection decisions that result in infeasible flows for the real network (fifth column) and that FBMC-GSK leads to a larger approximation error (fourth column) than FBMC-EP. We present the feasible domains of net positions for each model in Figure 2. It is interesting to observe that LMP and FBMC-EP clear with the same net positions. Nevertheless, the LMP acceptance/rejection decisions are feasible for the real network, whereas the decisions of FBMC-EP are not. This occurs because of the difference in price and location of bids within zone A. Zonal policies will accept these bids following the merit order, in the sense of accepting the bid at  $n_1$  fully before accepting any part of the bid at  $n_2$ . This decision, however, leads to overloading line  $l_{41}$ . According to FBMC-EP, this decision is feasible because there exists at least one  $\bar{v}$  with the same net positions (for instance, the optimal decision of the LMP policy).

FBMC-GSK clears with a cross-border exchange schedule that is infeasible for the real network. Note also that the set  $\mathcal{P}^{FB-GSK}$  does not include a slice of  $\mathcal{P}^{FB-EP}$  (containing feasible net positions for the real

Figure 1. (Color online) Four-Node, Three-Zone Network Data of Section 2.4



		Generators		Consumers	
$g$	$n(g)$	$Q_g$ [MW]	$P_g$ [\$/MWh]	$n$	$Q_n$ [MW]
1	$n_1$	500	8	$n_1$	300
2	$n_2$	200	45	$n_2$	300
3	$n_3$	300	18	$n_3$	300
4	$n_4$	500	200	$n_4$	300

Note. All lines have equal impedance.

**Table 1.** Summary of Clearing Quantities for a Case of Interzonal Congestion ( $l_{41}$  Limited to 100 MW)

Policy	Total cost (\$)	Absolute Error flow approx. (MW)	Overload $l_{41}$ (MW)
LMP	15,200	0	0
FBMC-GSK	7,217	475	79
FBMC-EP	7,800	300	50
ATCMC-EP	23,208	–	50

Notes. Flow approximation absolute error refers to the sum over all lines of the difference between model flows (i.e., flows inside the definitions of  $\mathcal{P}^{FB-GSK}$  in (7) and of  $\mathcal{P}^{FB-EP}$  in (8)) and implied flows (i.e., flows that would transit over the lines in the network if the optimal decisions of each policy  $v^*$  were implemented).

network) shaded with horizontal gray lines in Figure 2. In other words, FBMC-GSK fails to accurately account for cross-border exchanges and distorts the market outcome because of the discretionary parameters used for approximating power flows on lines.

**2.4.2. Intrazonal Scarce Transmission Capacity.** In order to study the effect of intrazonal congestion, we use the same system of Figure 1, where we now constrain the thermal capacity of line  $l_{12}$  to 100 MW and assume an unlimited capacity for all other lines. We employ the same GSKs as in the previous subsection.

We can observe in Table 2 that all zonal policies clear with acceptance/rejection decisions that are infeasible for the real network. As in the case of interzonal congestion, the flows estimated by FBMC-GSK are a less accurate approximation than those

**Table 2.** Summary of Clearing Quantities for a Case of Intrazonal Congestion ( $l_{12}$  Limited to 100 MW)

Policy	Total cost (\$)	Absolute error flow approx. (MW)	Overload $l_{12}$ (MW)
LMP	10,267	0	0
FBMC-GSK	5,800	536	150
FBMC-EP	5,800	300	150
ATCMC-EP	9,750	–	108

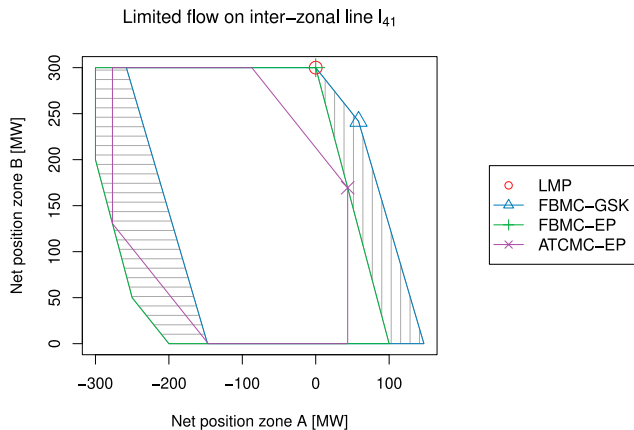
estimated by FBMC-EP. Interestingly, the estimated flows in FBMC-GSK can be in the opposite direction of the flows implied by the direct current power flow equations. As shown in Figure 3, for this case  $\mathcal{P}^{FB-GSK}$  turns out to be a relaxation of  $\mathcal{P}^{FB-EP}$ .

In summary, zonal markets fail to properly allocate scarce transmission capacity both when interzonal and intrazonal congestion arises. FBMC-EP outperforms FBMC-GSK in accuracy while not introducing market distortions. For this reason, in what follows, we will only consider FBMC-EP and will refer to it simply as FBMC. Similarly, we refer to ATCMC-EP simply as ATCMC.

### 3. Cutting-Plane Algorithms for Market Clearing Under the N-1 Security Criterion

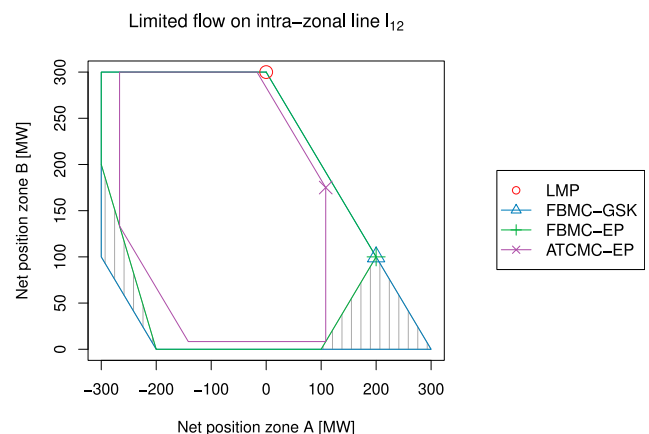
Electricity market operations ensure reliability by protecting the system against two types of uncertainty: (i) unpredictable changes in supply or demand, and (ii) contingencies related to unplanned outages of certain system elements. A commonly employed rule of thumb for ensuring reliable system

**Figure 2.** (Color online) Set of Feasible Net Positions on Plane A-B for a Case of Interzonal Congestion ( $l_{41}$  Limited to 100 MW)



Notes. The net position of zone C is implied by the net positions of A and B because of energy balance. The points indicate the zonal net positions at the optimal solution for each policy. The area shaded with horizontal gray lines corresponds to  $\mathcal{P}^{FB-EP} - \mathcal{P}^{FB-GSK}$  (feasible net positions prohibited in FBMC-GSK) and the area shaded with vertical gray lines corresponds to  $\mathcal{P}^{FB-GSK} - \mathcal{P}^{FB-EP}$  (infeasible net positions allowed in FBMC-GSK).

**Figure 3.** (Color online) Set of Feasible Net Positions on Plane A-B for a Case of Intrazonal Congestion ( $l_{12}$  Limited to 100 MW)



Notes. The points indicate the zonal net positions at the optimal solution for each policy. The area shaded with vertical gray lines corresponds to  $\mathcal{P}^{FB-GSK} - \mathcal{P}^{FB-EP}$ .

operation is the N-1 security criterion (Regulation (EU) 2017/1485), (CAISO 2015, Grid Optimization Competition 2018), whereby network operators set reserve targets in order to protect the system against generating unit outages and branch outages. The N-1 security criterion interacts with European day-ahead market clearing, and it is necessary to account for this interaction in order to produce results with policy relevance in a case study.<sup>3</sup> This is the main motivation for extending our models to N-1 robustness in the present section. A secondary motivation of this section is to demonstrate that our modeling framework is sufficiently flexible to include particular idiosyncrasies of zonal markets. Another example of a feature that can be easily accounted for within our modeling framework is strict linear pricing (which is the European approach for dealing with the pricing of nondivisibilities), to which our models are extended in Section EC.3 of the electronic companion.

Modeling generation contingencies in the case of LMP is more complicated. One way to model generation contingencies in a nodal setting is to use so-called “participation factors” (Grid Optimization Competition 2018). Participation factors are used for representing primary reserves (droop control and automatic generation control, that is, primary and secondary reserve in EU nomenclature), whereas operating reserves (which correspond to tertiary reserves in EU nomenclature) are represented in both the zonal and nodal models through reserve requirements. We therefore avoid double counting this level of security in the system by only including transmission line contingencies in the nodal and zonal day-ahead market clearing models. Notwithstanding, our real-time simulations also account for generator failures.

The algorithms that we develop in this section have been inspired by the algorithm proposed by Street et al. (2014) for security-constrained unit commitment. In this work, the authors use a cutting-plane procedure in order to progressively improve an under-approximation of the worst-case curtailment of demand after a contingency as a function of the commitment decisions, while considering dispatch decisions as a recourse. In contrast, our algorithms generate (i) descriptions of the feasible set of injections for LMP, considering dispatch decisions as first-stage variables, and (ii) descriptions of the inclusion Constraints (6) and (11). We base these descriptions on distance functions that become zero if and only if the corresponding inclusion constraints are respected. In what follows, Subsection 3.1 presents our cutting-plane algorithm for solving (1)–(3) and Subsection 3.2 presents a similar technique for solving (4)–(6), under the N-1 security criterion. Proofs for the propositions presented in this section and an algorithm for

solving (9)–(11), which uses the same ideas as the algorithm of Section 3.2, are presented in Section EC.1 of the electronic companion.

### 3.1. Decomposition Algorithm for Nodal Electricity Markets with N-1 Security

Following current industry standards (Grid Optimization Competition 2018), we define N-1 security for LMP markets as the ability of a system to withstand any single-element transmission contingency, while maintaining its current nodal injections and without violating any operating limits. The nodal injection  $r_n$  at node  $n$  corresponds to  $\sum_{g \in G(n)} Q_g v_g - Q_n$  and the security constraints correspond to generation and transmission limits. A nodal electricity market under the N-1 security criterion can then be cleared by solving

$$\min_{v \in [0,1], r} \sum_{g \in G} P_g Q_g v_g, \quad (14)$$

$$\text{s.t.} \quad \sum_{g \in G(n)} Q_g v_g - r_n = Q_n \quad \forall n \in N \quad [\rho_n], \quad (15)$$

$$r \in \mathcal{R}_{N-1}, \quad (16)$$

where  $\mathcal{R}_{N-1}$  is the feasible set of injections under any single-element transmission contingency, that is,  $\mathcal{R}_{N-1} = \bigcap_{\substack{m \in \{0,1\}^{|L|} \\ \|u\|_1 \leq 1}} \mathcal{R}(u)$  with

$$\mathcal{R}(u) = \left\{ \bar{r} \in \mathbb{R}^n \mid \exists (f, \theta) \in \mathbb{R}^{|L|} \times \mathbb{R}^{|N|} : \sum_{l \in L(n, \cdot)} f_l - \sum_{l \in L(\cdot, n)} f_l = \bar{r}_n \quad \forall n \in N, -F_l \leq f_l \leq F_l, f_l = B_l(1 - u_l)(\theta_{m(l)} - \theta_{n(l)}) \quad \forall l \in L \right\}. \quad (17)$$

The main idea behind our decomposition algorithm for LMP under N-1 security is to replace the inclusion Constraint (16) by a polyhedral outer approximation that is tight at the optimal solution  $(v^*, r^*)$ . This polyhedral outer approximation can be expressed as  $\{r \in \mathbb{R}^n \mid \sum_{m \in N} V_{m,n} r_n \leq W_m \quad \forall m = 1, \dots, M\} \supseteq \mathcal{R}_{N-1}$ , where  $M$  is the number of hyperplanes of the approximation. Following this reasoning, we propose clearing the market under LMP using Algorithm 1, which is based on repeatedly calling two oracles:

- A nodal market-clearing oracle  $NMCO(V, W)$  that, for a given  $V \in \mathbb{R}^{M \times |N|}$  and  $W \in \mathbb{R}^M$ , solves the relaxed LMP clearing problem ((14), (15),  $Vr \leq W$ ) and returns a vector of optimal nodal injections  $r^*$ .
- An injection oracle  $IO(r)$  that, for a given vector of nodal injections  $r$ , either certifies that  $r \in \mathcal{R}_{N-1}$  or returns a hyperplane that separates  $r$  from  $\mathcal{R}_{N-1}$ .

**Algorithm 1** Cutting-Plane Algorithm for Solving LMP Under N-1 Security

- 1: Initialize  $V := 0_{1,|N|}$ ,  $W := 0$ , inclusion := FALSE
- 2: **while** !inclusion **do**
- 3:   Call  $NMCO(V, W) \rightarrow r$
- 4:   Call  $IO(r) \rightarrow$  inclusion,  $(v, w)$
- 5:    $V := [V^T \ v]^T$ ,  $W := [W^T \ w]^T$
- 6: **end while**
- 7: Terminate: inner model of  $NMCO(V, W)$  gives the optimal clearing.

Although the market clearing oracle operations are clearly defined (they consist of solving a linear program), there are several ways in which we could devise an injection oracle; the effectiveness of Algorithm 1 in handling realistic instances will depend on the specific injection oracle that we employ. For example, an oracle that produces a deep separating hyperplane but relies on checking all N-1 contingencies one-by-one would not be effective in practice. With this in mind, we design our injection oracle based on the observation that (16) can be described equivalently in terms of a point-to-set distance function, that is,  $r \in \mathcal{R}_{N-1}$  if and only if  $d(r, \mathcal{R}_{N-1}) = 0$  for any distance function  $d$ . Concretely, given the definition of  $\mathcal{R}_{N-1}$ , we consider the following distance function:

$$d(r, \mathcal{R}_{N-1}) = \max_{\substack{u \in \{0,1\}^{|L|} \\ \|u\|_1 \leq 1}} \min_{\bar{r} \in \mathcal{R}(u)} \|r - \bar{r}\|_1,$$

which is defined using a bilevel mathematical program. The inner problem can be cast as a linear program that we can dualize and derive an alternative definition of  $d(\bar{r}, \mathcal{R}_{N-1})$  as a bilinear program:

$$\begin{aligned} d(r, \mathcal{R}_{N-1}) = \max_{u, \gamma, \phi, \rho} & - \sum_{n \in N} r_n \rho_n - \sum_{l \in L} F_l (\gamma_l^- + \gamma_l^+) \\ \text{s.t.} & -1 \leq \rho_n \leq 1 \quad \forall n \in N \\ & -\gamma_l^- + \gamma_l^+ + \phi_l - \rho_{n(l)} + \rho_{m(l)} = 0 \quad \forall l \in L \\ & \sum_{l \in L(n, \cdot)} B_l (1 - u_l) \phi_l + \sum_{l \in L(\cdot, n)} B_l \\ & \quad \cdot (1 - u_l) \phi_l = 0 \quad \forall n \in N \\ & \gamma \geq 0, u \in \{0,1\}^{|L|}, \|u\|_1 \leq 1. \end{aligned} \tag{18}$$

We then employ an injection oracle based on distance (IOD) in the implementation of Algorithm 1, which performs the following operations for every query point  $r$ :

1. Compute  $\tilde{w} := d(r, \mathcal{R}_{N-1})$  and obtain a subgradient  $v \in \partial_r d(r, \mathcal{R}_{N-1})$  ( $v$  corresponds to  $-\rho^*$ ).
2. If  $\tilde{w} = 0$ , then return TRUE,  $(0_{|N|}, 0)$ .
3. Else return FALSE,  $(v, -\tilde{w} + v^T r)$ .

Using IOD we can prove the following:

**Proposition 1.** Algorithm 1 terminates with an optimal solution in a finite number of iterations when using IOD as injection oracle.

Note that we do not need to solve (18) as a bilinear program when computing  $d(r, \mathcal{R}_{N-1})$ . Instead, we can use a mixed integer linear reformulation where the products between variables are relaxed using their McCormick envelopes (McCormick 1976). Because  $u$  is binary, this is an exact relaxation. Then IOD avoids exhaustively checking all N-1 contingencies; it only checks those that show promise within a branch-and-bound scheme. We further speed up IOD by allowing it to return suboptimal solutions to (18) as long as their value exceeds a positive cutoff, thereby also providing an infeasibility certificate and a valid separating hyperplane. Incorporating these improvements, IOD achieves practical performance on instances of realistic scale, such as those considered in the case study of Section 4.

**3.2. Decomposition Algorithm for Flow-Based Market Coupling with N-1 Security**

The notion of N-1 security in zonal markets requires that systems be able to withstand any single-element transmission contingency, while maintaining zonal net positions, without violating any security constraints (RTE 2019, 50Hertz et al. 2017). Note that this notion allows for remedial actions that preserve net positions following a transmission contingency, which is in contrast with the current practice in nodal markets, where no remedial actions are considered.

The FBMC problem under N-1 security can then be posed as ((4), (5)),  $p \in \mathcal{P}_{N-1}^{FB-EP} = \bigcap_{\substack{u \in \{0,1\}^{|L|} \\ \|u\|_1 \leq 1}} \mathcal{P}^{FB-EP}(u)$ , where  $\mathcal{P}_{N-1}^{FB-EP}$  is the feasible net position domain under any single-element transmission contingency and  $\mathcal{P}^{FB-EP}(u)$  corresponds to

$$\begin{aligned} \mathcal{P}^{FB-EP}(u) = \left\{ p \in \mathbb{R}^{|Z|} \mid \exists (\bar{v}, f, \theta) \in [0, 1]^{|G|} \times \mathbb{R}^{|N|} \times \mathbb{R}^{|L|} : \right. \\ \sum_{g \in G(z)} Q_g \bar{v}_g - p_z = \sum_{n \in N(z)} Q_n \quad \forall z \in Z, \\ \sum_{g \in G(n)} Q_g \bar{v}_g - \sum_{l \in L(n, \cdot)} f_l + \sum_{l \in L(\cdot, n)} f_l = Q_n \quad \forall n \in N, \\ \left. -F_l \leq f_l \leq F_l, f_l = B_l (1 - u_l) (\theta_{m(l)} - \theta_{n(l)}) \quad \forall l \in L \right\}. \end{aligned}$$

This formulation of the FBMC clearing problem under N-1 security ensures that the market clears with a net position that (i) is feasible under the no-contingency case and (ii) that can be maintained through remedial actions under any single-element transmission contingency. This definition of the flow-based domain also implies that the feasible sets of net positions may



differ between zonal and nodal markets under N-1 security, a result that we formalize in Proposition 2. In words, this proposition implies that the nodal N-1 security criterion imposes more conservative limits on interzonal exchanges than its zonal counterpart, according to the current regulation of European markets.

**Proposition 2.** Let  $\mathcal{P}_{N-1}^{LMP}$  be the feasible set of zonal net positions of the nodal market under N-1 security, that is, the projection of  $\{(v, r) \in [0, 1]^{|G|} \times \mathbb{R}^{|N|} \mid (15), (16)\}$  onto the zonal net position space. Then  $\mathcal{P}_{N-1}^{LMP} \subseteq \mathcal{P}_{N-1}^{FB-EP}$ .

We solve the FBMC clearing problem under N-1 security using an analogous strategy to the one used for nodal markets in the previous section. Concretely, we replace the inclusion constraint  $p \in \mathcal{P}_{N-1}^{FB-EP}$  by a polyhedral outer approximation,  $\sum_{z \in Z} V_{m,z} p_z \leq W_m \forall m = 1, \dots, M$ , which is tight at the optimal solution  $p^*$ . The outer approximation is progressively constructed by querying the distance function

$$d(p, \mathcal{P}_{N-1}^{FB-EP}) = \max_{\substack{u \in \{0,1\}^{|L|} \\ \|u\|_1 \leq 1}} \min_{\bar{p} \in \mathcal{P}_{N-1}^{FB-EP}(u)} \|p - \bar{p}\|_1, \quad (19)$$

which becomes zero if and only if  $p \in \mathcal{P}_{N-1}^{FB-EP}$ . The evaluation of this distance function requires solving a mixed-integer linear program, from the solution of which we can generate a separating hyperplane whenever  $p \notin \mathcal{P}_{N-1}^{FB-EP}$ . Then, we follow the procedure described in Algorithm 1 for solving the FBMC clearing problem under N-1 security, replacing NMCO and IO, respectively, with

- a zonal market-clearing oracle  $ZMCO(V, W)$  that, for a given  $V \in \mathbb{R}^{M \times |Z|}$  and  $W \in \mathbb{R}^M$ , solves the FBMC clearing problem using  $Vp \leq W$  as a substitute for  $p \in \mathcal{P}_{N-1}^{FB-EP}$  and returns a vector of optimal net positions  $p^*$  and
- a net position oracle based on distance  $NPOD(p)$  that, for a given vector of net positions  $p$  evaluates  $d(p, \mathcal{P}_{N-1}^{FB-EP})$  and either certifies that  $p \in \mathcal{P}_{N-1}^{FB-EP}$  or returns a hyperplane that separates  $p$  from  $\mathcal{P}_{N-1}^{FB-EP}$ .

The resulting algorithm can be proven to terminate finitely with the optimal market clearing solution or an infeasibility certificate, by the same arguments used to prove the finite termination of Algorithm 1.

## 4. Simulation Setup

In the case study, of the following section, we simulate a generalization of the day-ahead markets for LMP, FBMC, and ATCMC that were presented in Section 2. The generalized formulations additionally consider commitment (on-off) decisions for slow generators,<sup>4</sup> reserves, European pricing restrictions for nondivisible bids that correspond to the commitment

of resources and the N-1 security criterion. We assume co-optimization of energy and reserve in the day-ahead market, which differs from the current implementation of the market in Europe where the reserve market can be cleared before, simultaneously, or after the energy market. We adopt this assumption in order to focus on quantifying the impact of zonal pricing on unit commitment. The assumption corresponds to a best-case version of the commitment of reserve.

We simulate real-time markets for managing congestion and balancing the system after renewable energy forecast errors and transmission and generation outages have been revealed. Real-time markets must respect the commitment of slow generators, which is decided in the day-ahead market. Moreover, in the case of zonal markets, real-time balancing strives to maintain the cleared net position of each zone. As mentioned in the introduction, these real-time models also correspond to optimistic versions of current European practices in which congestion management and balancing are performed separately. The reader is referred to EC.2 in the electronic companion for a detailed presentation of these two-settlement models.

We use a modified version of the CWE instance of Aravena and Papavasiliou (2017) consisting of (i) 346 slow generators with a total capacity of 154 GW; (ii) 301 fast thermal generators with a total capacity of 89 GW; (iii) 1,312 renewable generators with a total capacity of 149 GW; (iv) 632 buses; and (v) 945 branches (3,491 individual circuits).<sup>5</sup> The average demand of the system amounts to 134 GW.

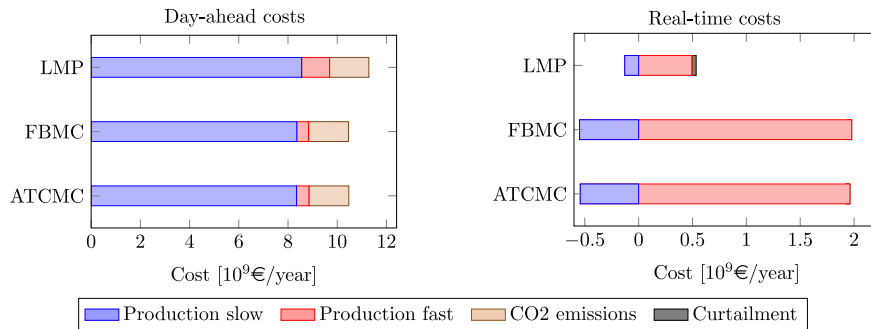
We consider 768 typical snapshots for day-ahead market clearing. Each snapshot corresponds to different demand, renewable forecasts, and maintenance schedules (deratings) for thermal generators. For each snapshot, we generate 1,150 random realizations of uncertainty (renewable forecast errors, forced outages of thermal generators, and forced outages of transmission lines) in order to simulate real-time operation. For generators and lines, forced outages are randomly generated based on Bernoulli distributions, that is, each element is completely unavailable with a probability equal to its forced outage rate, otherwise the element is fully available (up to derating

**Table 3.** Total Costs and Cost Performance Comparison Between Policies

Policy	Day-ahead (€/year)	Real-time (€/year)	Total (€/year)	Efficiency losses
Perfect foresight	–	11,476	11,476	–2.90%
LMP	11,284	534	11,818	–
FBMC	10,458	1,963	12,420	5.09%
ATCMC	10,470	1,949	12,419	5.08%

Note. Efficiency losses measured with respect to LMP total cost.

**Figure 4.** (Color online) Breakdown of Costs in Day-Ahead Market and Real-Time Operations for the Three Policies Under Investigation



Note. Real-time costs only account for the differences with respect to day-ahead values.

from maintenance schedules). In total, we consider 883,200 different operating conditions for each policy. Considering that each snapshot corresponds to an hour of operation, our simulations correspond to approximately 100 years of operation.

### 5. Results and Discussion

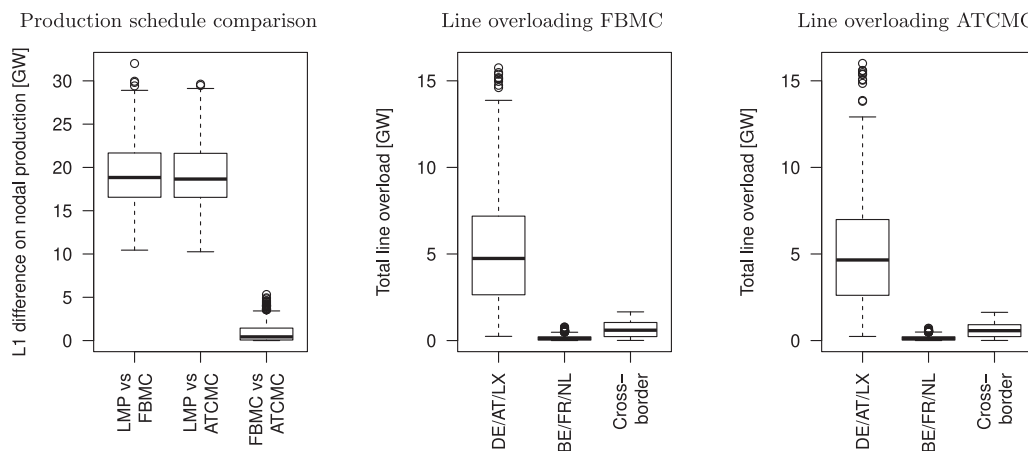
We present a comparison between LMP, FBMC, and ATCMC in terms of their day-ahead and real-time performance. Table 3 presents the overall costs of each policy at each stage. The table also contains the perfect foresight (PF) benchmark, which is an unreachable performance benchmark. PF and LMP show important cost differences mainly because of (i) the ability of PF to adapt the commitment of slow units between different realizations of uncertainty and (ii) out-of-merit commitment decisions made by LMP in order to satisfy the N-1 security criterion. In particular, LMP spreads out production through the system in order to obtain nodal net injections that are

feasible against any single-element transmission contingency, leading to commitment decisions that are inefficient for scenarios with zero or many simultaneous outages.

LMP exhibits larger day-ahead costs than the zonal designs FBMC and ATCMC, which attain very similar costs at all stages (differences between FBMC and ATCMC are within the termination gap of the corresponding day-ahead models). At the same time, the real-time costs of FBMC and ATCMC are notably greater than those of LMP. As indicated in Figure 4, this difference stems mostly from the use of fast thermal generators (e.g., gas and oil) in real time by FBMC and ATCMC. The inefficient deployment of these units drives the difference in cost performance between zonal and nodal markets to about 5.1% of the total operation costs (which corresponds to approximately €600 million/year for the CWE).

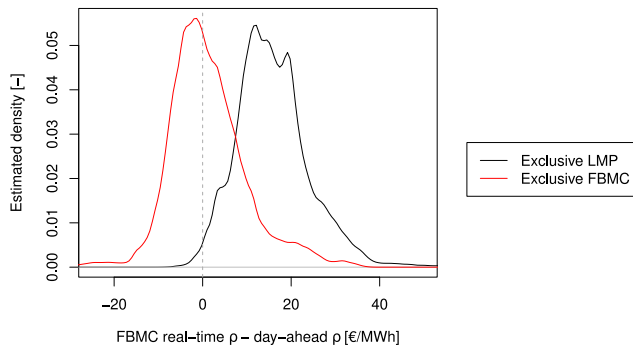
In addition to achieving a similar cost performance, FBMC and ATCMC result in similar acceptance/

**Figure 5.** Production Schedule and Line Overloading Comparison Between the Different Market Clearing Policies



Notes. The left box plot presents the distribution of the absolute deviation between the day-ahead production schedules of the three different policies over all snapshots. The center and right box plots present the overloading pattern caused by the acceptance/rejection decisions of FBMC and ATCMC.

**Figure 6.** (Color online) Distribution of Geographical Averages of Marginal Cost Differences Between Real Time and Day Ahead for FBMC



*Notes.* This figure has been obtained without enforcing zonal net positions in real-time. For a given snapshot and a given realization of uncertainty, the “exclusive LMP” series is computed by averaging the differences  $\rho_n^{RT} - \rho_{z(n)}^{DA}$  over all nodes where LMP committed slow units and FBMC did not commit units, weighted by the capacity committed exclusively by LMP. The exclusive FBMC series is computed analogously.

rejection decisions and implied flows. This is indicated in Figure 5. The center and right box plots of Figure 5 demonstrate that FBMC and ATCMC overload both internal and interzonal lines, with similar overloading patterns. This behavior was already observed in the four-node network in Tables 1 and 2 and is attributed to the fact that zonal merit order dispatch results in similar nodal injections in both models. Zonal merit order overlooks the implications of nodal injections on power flows, thereby failing at allocating transmission capacity.

The differences between FBMC and LMP are driven by the same factors that drive the differences between ATCMC and LMP that are observed in the literature (Ehrenmann and Smeers 2005, Aravena and Papavasiliou 2017). The major factor contributing to the inefficiency of FBMC is the suboptimal commitment decisions of this policy. In order to isolate this factor, we simulate the real-time market without imposing the requirement of maintaining zonal day-ahead net positions and record the dual variables of the power balance constraints  $\rho^{RT}$ . We observe in Figure 6 that in the majority of cases where LMP commits a unit at a certain location  $n$  in the day ahead and FBMC does not,  $\rho_n^{RT}$  becomes larger than the corresponding day-ahead zonal price  $\rho_{z(n)}^{DA}$ , indicating the need for generation at  $n$ . On the other hand, whenever FBMC commits at a certain location  $n$  in the day ahead and LMP does not, we observe that  $\rho_n^{RT}$  can be smaller or larger than  $\rho_{z(n)}^{DA}$ , depending on forecast errors and forced outages, indicating that generation capacity is not systematically required at the given location. FBMC fails at recognizing these locational differences as a direct consequence

of the zonal aggregation in the day-ahead market. We quantify the efficiency losses of FMBC caused by suboptimal commitment at 3.05% of the total operation costs. The remaining 2.04% cost difference is explained by the requirement of maintaining day-ahead net positions in the presence of renewable forecast errors in FBMC, whereas LMP is able to exploit cross-zonal balancing.

## 6. Conclusions

We present models for flow-based market coupling and for available-transfer-capacity market coupling that do not depend on discretionary parameters and are based purely on the technical parameters of the grid. We analyze the implications of these models on a four-node instance and a realistic-scale instance of the CWE system. In both instances, we observe that both zonal market designs encounter challenges in allocating the transmission capacity of interzonal lines and intrazonal lines because of the loss of locational information.

These deficiencies affect the real-time performance of the system, leading to efficiency losses of 5.09% for flow-based market coupling and 5.08% for available-transfer-capacity market coupling with respect to a nodal market design. The similarities that are unveiled between both zonal designs raise the question of whether flow-based market coupling should be expanded to cover other zones of Europe, especially when certain zones, such as Poland, are already planning to switch to a nodal market design (PSE SA 2017).

Future extensions of the present work will focus on the impact of the flow-based model with exact projection on prices and on the study of the meaning of these prices as they relate to investment.

## Acknowledgments

The authors thank Mr. Alain Marien of the Commission de Régulation de l'Électricité et du Gaz and Dr. Gauthier de Maere d'Aertrycke (Engie) for their helpful comments and discussions during the development of this work. The authors also thank Gurobi and FICO for providing distributed academic licenses for Gurobi and Xpress, respectively; the Lawrence Livermore National Laboratory for providing computing time at the Cab cluster; and the Consortium des Équipements de Calcul Intensif for providing computing time at the Lemaitre2 cluster.

## Endnotes

<sup>1</sup>The flow reliability margin is a parameter that is used by TSOs in order to decrease the capacity of critical branches that are offered to the market. The role of flow reliability margins is to account for uncertainties during the capacity calculation process (i.e., uncertainties linked to the definition of the base case or to the simplified network representation).

<sup>2</sup>In what concerns the firmness of cross-border capacity, we note that the new Regulation (EU) 2019/943 requires instead that 70% of the capacity of the lines be made available to the market, even if this implies using cross-border redispatch in order to support the cleared net positions. An analysis of the implications of this new rule is outside the scope of the present paper. Instead, we consider in this paper the principle of firmness of cross-border capacity, as described in Regulation (EU) 2015/1222.

<sup>3</sup>The influence of N-1 security on the FBMC model used in the day-ahead European market clearing model can be appreciated when analysing historical data of the flow-based constraints that are used as input for the market coupling process. These constraints are publicly available online (<https://www.jao.eu/>). At the time of writing (February 11, 2020), 89% of the constraints were associated to a contingency. More evidence of the importance of the security criterion for providing results with policy relevance can be found in the first edition of the bidding zone review. In the review, the participants mention the absence of N-1 security as a reason for the failure of the model-based bidding zone configuration proposals.

<sup>4</sup>We refer to slow generators as generators with a unit commitment schedule that needs to be fixed in the day-ahead time frame and cannot be changed in real time. Concretely, these correspond to coal and nuclear units.

<sup>5</sup>Each N-1 transmission contingency corresponds to the forced outage of a single circuit.

## References

- 50Hertz, Amprion, APG, Creos, Elia, EPEXSpot, RTE, TenneT, Transnet BW (2017) Documentation of the CWE FB MC solution. Accessed April 9, 2021, <https://www.creg.be/sites/default/files/assets/Consult/2019/1891/PRD1891Annex1.pdf>.
- Agency for the Cooperation of Energy Regulators (ACER) (2018) Annual report on the results of monitoring the internal electricity and natural gas markets in 2017. Report ACER, Ljubljana, Slovenia.
- Agency for the Cooperation of Energy Regulators (ACER) (2019) Monitoring report on the implementation of the CACM regulation and the FCA regulation. Report ACER, Ljubljana, Slovenia.
- Amprion, APG, Creos, Elia, RTE, TenneT, Transnet BW (2015) CWE flow based market-coupling project: Parallel run performance report. Accessed April 9, 2021, <https://www.jao.eu/support/resourcecenter/overview?parameters=%7B%22IsCWEFBMCRelevantDocumentation%22%3A%22True%22%7D>.
- APX Group, Belpex, Powernext (2006) Trilateral market coupling algorithm. Accessed April 9, 2021, [https://inis.iaea.org/collection/NCLCollectionStore/\\_Public/38/045/38045712.pdf](https://inis.iaea.org/collection/NCLCollectionStore/_Public/38/045/38045712.pdf).
- APX Group, Belpex, Cegedel Net, EEX, ELIA Group, EnBw, E-On Netz, Powernext, RTE, RWE, TenneT (2010) A report for the regulators of the Central West European (CWE) region on the final design of the market coupling solution in the region, by the CWE MC Project. Accessed April 9, 2021, [http://www.epexspot.com/en/market-coupling/documentation\\_cwe](http://www.epexspot.com/en/market-coupling/documentation_cwe).
- Aravena I, Papavasiliou A (2017) Renewable energy integration in zonal markets. *IEEE Trans. Power Systems* 32(2): 1334–1349.
- Ben-Tal A, El Ghaoui L, Nemirovski A (2009) *Robust Optimization*, Princeton Series in Applied Mathematics (Princeton University Press, Princeton, NJ).
- California Independent System Operator (CAISO) (2015) Business Practice Manual for Market Operations (version 45).
- Commission de Régulation de l'Électricité et du Gaz (CREG) (2017) Functioning and design of the Central West European day-ahead flow based market coupling for electricity: Impact of TSOs discretionary actions. Report CREG, Brussels, Belgium.
- Dierstein C (2017) Impact of generation shift key determination on flow based market coupling. *14th Internat. Conf. Eur. Energy Market (EEM)*, Dresden, Germany, 1–7. doi: 10.1109/EEM.2017.7981901.
- Ehrenmann A, Smeers Y (2005) Inefficiencies in European congestion management proposals. *Utilities Policy* 13(2):135–152.
- Energy Markets Inspectorate (EI, Sweden), Norwegian Water Resources and Energy Directorate (NVE) (2017) Reduced capacity on German-Nordic interconnectors, regulatory framework and socioeconomic effects on the European electricity market. Report. Accessed January 8, 2021, [https://ei.se/Documents/Nyheter/Nyheter%202017/Rapport\\_EI\\_NVE\\_Reduced%20interconnector%20capacity\\_170616.pdf](https://ei.se/Documents/Nyheter/Nyheter%202017/Rapport_EI_NVE_Reduced%20interconnector%20capacity_170616.pdf).
- European Commission (2015) Commission Regulation (EU) 2015/1222 of July 24, 2015 establishing a guideline on capacity allocation and congestion management.
- European Commission (2017a) Commission Regulation (EU) 2017/1485 of August 2, 2017 establishing a electricity transmission system operation.
- European Commission (2017b) Commission Regulation (EU) 2017/2195 of November 23, 2017 establishing a guideline on electricity balancing.
- European Network of Transmission System Operators for Electricity (ENTSO-E) (2017) Statistical Factsheet 2016. Report ENTSO-E, Brussels, Belgium.
- European Network of Transmission System Operators for Electricity (ENTSO-E) (2018a) First edition of the bidding zone review: Final report. Report ENTSO-E, Brussels, Belgium.
- European Network of Transmission System Operators for Electricity (ENTSO-E) (2018b) ENTSO-E transparency platform. Accessed April 26, 2018, <https://transparency.entsoe.eu/>.
- European Parliament, Council of the European Union (2003) Regulation 1228/2003 of the European Parliament and of the Council of June 26, 2003 on conditions for access to the network for cross-border exchanges in electricity.
- European Parliament, Council of the European Union (2009) Regulation (EC) No 714/2009 of the European Parliament and of the Council of July 13, 2009 on conditions for access to the network for cross-border exchanges in electricity and repealing Regulation (EC) No 1228/2003.
- European Parliament, Council of the European Union (2019) Regulation (EU) No 2019/943 of the European Parliament and of the Council of 5 June 2019 on the internal market for electricity.
- Eurostat (2018) Population on 1 January. Accessed April 26, 2018, <http://ec.europa.eu/eurostat/tgm/table.do?language=en&pcode=tps00001>.
- Federal Energy Regulatory Commission (FERC) (2018) Market oversight, electric power markets. Accessed April 26, 2018, <https://www.ferc.gov/market-oversight/mkt-electric/overview.asp>.
- Grid Optimization Competition (2018) SCOPF problem formulation: Challenge 1. Accessed November 29, 2018, <https://gocompetition.energy.gov/challenges/challenge-1/formulation>.
- Hogan WW (2016) Virtual bidding and electricity market design. *Electricity J.* 29(5):33–47.
- Jensen TV, Kazempour J, Pinson P (2017) Cost-optimal ATCS in zonal electricity markets. *IEEE Trans. Power Systems* 33(4):3624–3633.
- Joint Allocation Office (2015) Yearly long term auctions. Accessed January 9, 2021, <https://www.jao.eu/>.
- Marien A, Luickx P, Tirez A, Woitrin D (2013) Importance of design parameters on flow-based market coupling implementation. *10th Internat. Conf. Eur. Energy Market (EEM)*, Stockholm, Sweden, 1–8.



- McCormick GP (1976) Computability of global solutions to factorable nonconvex programs: Part I—convex underestimating problems. *Math. Programming* 10(1):147–175.
- Papavasiliou A, Smeers Y, de Maere d’Aertrycke G (2019) Study on the general design of a mechanism for the remuneration of reserves in scarcity situations. Accessed January 9, 2021, <https://www.creg.be/sites/default/files/assets/Publications/Notes/Z1986Annex.pdf>.
- PSE SA (2017) PSE S.A. informs on the conclusion of the tendering procedure for the supply and implementation of the Electricity Balancing Market Management System in Poland. Accessed January 9, 2021, <https://www.pse.pl/web/pse-eng/-/pse-s-a-informs-on-the-conclusion-of-the-tendering-procedure-for-the-supply-and-implementation-of-the-electricity-balancing-market-management-system-i>.
- RTE Réseau de Transport d’Electricité (2019) Documentation technique de référence. Accessed January 9, 2021, [https://www.services-rte.com/files/live/sites/services-rte/files/documentsLibrary/01-11-19%20complet\\_fr\\_2730](https://www.services-rte.com/files/live/sites/services-rte/files/documentsLibrary/01-11-19%20complet_fr_2730).
- Schweppe F, Caramanis M, Tabors R, Bohn R (1988) *Spot pricing of electricity*. *Power Electronics and Power Systems* (Springer, New York), 357.
- Street A, Moreira A, Arroyo JM (2014) Energy and reserve scheduling under a joint generation and transmission security criterion: An adjustable robust optimization approach. *IEEE Trans. Power Systems* 29(1):3–14.
- TenneT (2014) Determining securely available cross-border transmission capacity. Accessed April 9, 2021, [https://www.tennet.eu/fileadmin/user\\_upload/The\\_Electricity\\_Market/Transparency/SO-000\\_15-000\\_Determining\\_securely\\_available\\_cross-border\\_transmission\\_capacity\\_18052015.pdf](https://www.tennet.eu/fileadmin/user_upload/The_Electricity_Market/Transparency/SO-000_15-000_Determining_securely_available_cross-border_transmission_capacity_18052015.pdf).
- Van den Bergh K, Boury J, Delarue E (2016) The flow-based market coupling in central western Europe: Concepts and definitions. *Electricity J.* 29(1):24–29.
- Wanik D, Rehtanz C, Handschin E (2010) Flow-based evaluation of congestions in the electric power transmission system. *7th Internat. Conf. Eur. Energy Market (EEM)*, Madrid, Spain, 1–6. doi: 10.1109/EEM.2010.5558762.

---

**Ignacio Aravena** received BSc and MSc degrees in electrical engineering from the Federico Santa Maria Technical University, Valparaíso, Chile, and a PhD degree in applied mathematics from UCLouvain, Louvain-la-Neuve, Belgium. He is currently a member of the research staff at the Computational Engineering Division of the Lawrence Livermore National Laboratory, Livermore, California.

**Quentin Lété** obtained his BSc and MSc degrees in mathematical engineering from UCLouvain, Louvain-la-Neuve, Belgium. He is currently a PhD student on applied mathematics at the Louvain Institute of Data Analysis and Modeling in economics and statistics of UCLouvain, and he is a Research Fellow (*Aspirant*) of the Fonds de la Recherche Scientifique (FNRS).

**Anthony Papavasiliou** received a BSc degree in electrical and computer engineering from the National Technical University of Athens, Greece, and a PhD degree from the Department of Industrial Engineering and Operations Research at the University of California at Berkeley, Berkeley, California. He is an associate professor at UCLouvain, in Louvain-la-Neuve, Belgium, where he holds the ENGIE Chair Professorship 2018–2021 and is a member of the Louvain Institute of Data Analysis and Modeling.

**Yves Smeers** received MS and PhD degrees from Carnegie Mellon University, Pittsburgh, Pennsylvania. He is currently a professor emeritus and a member of the Louvain Institute of Data Analysis and Modeling at UCLouvain, Louvain-la-Neuve, Belgium.